MOLECULAR AND CELLULAR BIOLOGY, Jan. 2009, p. 435–447 Vol. 29, No. 2
0270-7306/09/$08.00+0 doi:10.1128/MCB.01144-08

Identification of G Protein α Subunit-Palmitoylating Enzyme▽

Ryouhei Tsutsumi,[1] Yuko Fukata,[1,2] Jun Noritake,[1] Tsuyoshi Iwanaga,[1] Franck Perez,[3,4] and Masaki Fukata[1,2]*

Division of Membrane Physiology, Department of Cell Physiology, National Institute for Physiological Sciences, Okazaki, Aichi 444-8787, Japan[1]; PRESTO, Japan Science and Technology Agency, Chiyoda, Tokyo 102-0075, Japan[2]; and Centre National de la Recherche Scientifique, Unité Mixte de Recherche 144,[3] and Institut Curie Section Recherche,[4] 75248 Paris Cedex 05, France

Received 20 July 2008/Returned for modification 14 August 2008/Accepted 29 October 2008

The heterotrimeric G protein α subunit (Gα) is targeted to the cytoplasmic face of the plasma membrane through reversible lipid palmitoylation and relays signals from G-protein-coupled receptors (GPCRs) to its effectors. By screening 23 DHHC motif (Asp-His-His-Cys) palmitoyl acyl-transferases, we identified DHHC3 and DHHC7 as Gα palmitoylating enzymes. DHHC3 and DHHC7 robustly palmitoylated $G\alpha_q$, $G\alpha_s$, and $G\alpha_{i2}$ in HEK293T cells. Knockdown of DHHC3 and DHHC7 decreased $G\alpha_{q/11}$ palmitoylation and relocalized it from the plasma membrane into the cytoplasm. Photoconversion analysis revealed that $G\alpha_q$ rapidly shuttles between the plasma membrane and the Golgi apparatus, where DHHC3 specifically localizes. Fluorescence recovery after photobleaching studies showed that DHHC3 and DHHC7 are necessary for this continuous $G\alpha_q$ shuttling. Furthermore, DHHC3 and DHHC7 knockdown blocked the α_{1A}-adrenergic receptor/$G\alpha_{q/11}$-mediated signaling pathway. Together, our findings revealed that DHHC3 and DHHC7 regulate GPCR-mediated signal transduction by controlling Gα localization to the plasma membrane.

G-protein-coupled receptors (GPCRs) form the largest family of cell surface receptors, consisting of more than 700 members in humans. GPCRs respond to a variety of extracellular signals, including hormones and neurotransmitters, and are involved in various physiologic processes, such as smooth muscle contraction and synaptic transmission (20, 25). Heterotrimeric G proteins, composed of α, β, and γ subunits, transduce signals from GPCRs to their effectors and play a central role in the GPCR signaling pathway (13, 21, 24, 32). Although the Gα subunit seems to localize stably at the cytosolic face of the plasma membrane (PM), a recent report suggested that $G\alpha_o$, a Gα isoform, shuttles rapidly between the PM and intracellular membranes (2). The PM targeting of Gα requires both interaction with the Gβγ complex and subsequent lipid palmitoylation of Gα (22). Thus, palmitoylation of Gα is a critical determinant of membrane targeting of the heterotrimer Gαβγ.

Protein palmitoylation is a common posttranslational modification with lipid palmitate and regulates protein trafficking and function (7, 18). Gα is a classic and representative palmitoyl substrate (19, 38), and recent studies revealed that protein palmitoylation modifies virtually almost all the components of G-protein signaling, including GPCRs, Gα subunits, several members of the RGS (regulators of G-protein signaling) family of GTPase-activating proteins, GPCR kinase GRK6, and some small GTPases (7, 33). This common lipid modification plays an important role in compartmentalizing G-protein signaling to the specific microdomain, such as membrane caveolae and lipid raft (26). The palmitoyl thioester bond is relatively labile, and palmitates on substrates turn over rapidly, allowing proteins to shuttle between the cytoplasm/intracellular organelles and the PM (2, 3, 27). For example, binding of isoproterenol to the β-adrenergic receptor markedly accelerates the depalmitoylation of the associated $G\alpha_s$, shifting $G\alpha_s$ to the cytoplasm (37). This receptor activation-induced depalmitoylation was also observed in a major postsynaptic PSD-95 scaffold, which anchors the AMPA (alpha-amino-3-hydroxy-5-methyl-isoxazole-4-propionic acid)-type glutamate receptor at the excitatory postsynapse through stargazin (6). On glutamate receptor activation, accelerated depalmitoylation of PSD-95 dissociates PSD-95 from postsynaptic sites and causes AMPA receptor endocytosis (6). Thus, palmitate turnover on $G\alpha_s$ and PSD-95 is accelerated by receptor activation, contributing to down-regulation of the signaling pathway. However, the enzymes that add palmitate to proteins (palmitoyl-acyl transferases [PATs]) and those that cleave the thioester bond (palmitoyl-protein thioesterases) were long elusive.

Recent genetic studies in *Saccharomyces cerevisiae* identified Erf2/Erf4 (1, 40) and Akr1 (29) as PATs for yeast Ras and yeast casein kinase 2, respectively. Erf2 and Akr1 have four- to six-pass transmembrane domains and share a common domain, referred to as a DHHC domain, a cysteine-rich domain with a conserved Asp-His-His-Cys signature motif. Because the DHHC domain is essential for the PAT activity, we isolated 23 mammalian DHHC domain-containing proteins (DHHC proteins) and developed a systematic screening method to identify the specific enzyme-substrate pairs (11, 12): DHHC2, -3, -7, and -15 for PSD-95 (11); DHHC21 for endothelial NO synthase (10); and DHHC3 and -7 for $GABA_A$ receptor γ2 subunit (9). Several other groups also reported that DHHC9 with GCP16 mediates palmitoylation toward H- and N-Ras (36) and that DHHC17, also known as HIP14, palmitoylates several neuronal proteins: huntingtin (14), SNAP-25, and CSP (14, 23, 35). However, the existence of PATs for Gα has been contro-

* Corresponding author. Mailing address: Division of Membrane Physiology, Department of Cell Physiology, National Institute for Physiological Sciences, 5-1 Higashiyama, Myodaiji, Okazaki, Aichi 444-8787, Japan. Phone: 81 564 59 5873. Fax: 81 564 59 5870. E-mail: mfukata@nips.ac.jp.

▽ Published ahead of print on 10 November 2008.

versial because spontaneous palmitoylation of Gα could occur in vitro (4).

In this study, we screened the 23 DHHC clones to examine which DHHC proteins can palmitoylate Gα. We found that DHHC3 and -7 specifically and robustly palmitoylate Gα at the Golgi apparatus. Inhibition of DHHC3 and -7 reduces $G\alpha_{q/11}$ palmitoylation levels and delocalizes it from the PM to the cytoplasm in HeLa cells and primary hippocampal neurons. Also, DHHC3 and -7 are necessary for the continuous $G\alpha_q$ shuttling between the Golgi apparatus and the PM. Finally, blocking DHHC3 and -7 inhibits the α_{1A}-adrenergic receptor [α_{1A}-AR]/$G\alpha_q$-mediated signaling pathway, indicating that DHHC3 and -7 play an essential role in GPCR signaling by regulating Gα localization.

MATERIALS AND METHODS

Cell culture and transfection. The drugs used were 2-bromohexadecanoic acid (2-bromopalmitate [2-BP]) (Fluka), cycloheximide (CHX; Sigma), phenylephrine (Sigma), and prazosin (Sigma). For transfection of plasmid DNA and small interfering RNA (siRNA) into HeLa or HEK293T cells, Lipofectamine Plus reagent and Lipofectamine 2000 (Invitrogen) were used, respectively. Cultured hippocampal neurons (2.5×10^4 cells) were seeded onto 12-mm coverslips in 24-well dishes. Neurons (DIV8) were transfected with pCAGGS-mCherry-miR (where mCherry is a fluorescent protein) vectors by Lipofectamine 2000.

Antibodies. The antibodies used were rabbit polyclonal antibodies to $G\alpha_{q/11}$ (Santa Cruz Biotechnology) and GODZ/DHHC3 (Abcam); mouse monoclonal antibodies to β-catenin (BD Biosciences), hemagglutinin ([HA] clone 12CA5 from Roche Applied Science and clone 16B12 from Covance), Lck (Chemicon), and GM130 (BD Biosciences); chicken polyclonal antibody to green fluorescent protein (GFP) (Chemicon); and rabbit monoclonal antibodies to CREB (Cell Signaling) and phospho-CREB Ser133 (pCREB) (Cell Signaling). Rabbit polyclonal antibodies to GFP and moesin were raised against glutathione *S*-transferase-GFP and glutathione *S*-transferase–moesin (amino acids 307 to 577), respectively.

Plasmid constructions. $G\alpha_q$-tagged with the fluorescent protein Dendra2 (Evrogen) (16) was made by replacing a GFP fragment of $G\alpha_q$-GFP, which was well characterized (15). $G\alpha_q$-Dendra2 stimulated phospholipase C in response to α_{1A}-AR activation (data not shown); it was palmitoylated by DHHC3 and -7 (data not shown) and was localized at the PM (Fig. 1A) as effectively as $G\alpha_q$-GFP. We concluded that $G\alpha_q$-Dendra2 is functional as endogenous $G\alpha_q$ and $G\alpha_q$-GFP. $G\alpha_{i2}$-GFP was constructed by inserting enhanced GFP (EGFP) with an SGGGGS linker at both the N and C ends between 114A and 115G of $G\alpha_{i2}$. pEF-Bos-HA-mouse DHHC (mDHHC) clones were described previously (11). Dendra2-DHHC3 and FLAG-DHHC3 were constructed by subcloning cDNA of DHHC3 into pDendra2-C and pCAGGS-FLAG, respectively. DHHC3 with the mutation C157S [DHHC3(C157S)], DHHC7(C160S), and $G\alpha_q$ with mutations of cysteines 9 and 10 to serine [$G\alpha_q$ (CS)] were generated using site-directed mutagenesis. To mark the Golgi compartment position, EGFP of galactosyl transferase (GalT)-EGFP (16, 34) was replaced with mCherry. α_{1A}-AR (accession number NM013461) was cloned from mouse brain cDNA by reverse transcription-PCR (RT-PCR) and subcloned into pcDNA3.1 with sequence for a FLAG tag at the 5′ end. For knockdown of DHHC2 and -3 in hippocampal neurons, we used an miR-RNA interference (RNAi) system (Invitrogen). The following targeting sequences were used: DHHC2, GGTGAACAATTGTGTTGGATT; and DHHC3, TGAGACGGGAATAGAACAATT. After these oligonucleotides were subcloned into pcDNA6.2-EmGFP-miR (Invitrogen), EmGFP was replaced with mCherry, and the pre-microRNA expression cassette of pcDNA6.2-mCherry-miR was transferred to pCAGGS vector with β-actin promoter. The validity of knockdown vectors was confirmed by specific antibodies (data not shown). EGFP-CAAX, which encodes a polybasic region and CAAX motif of K-Ras, was generated by inserting a synthetic DNA fragment obtained by annealing the sense synthetic nucleotide 5′-GATCCAAGATGAGCAAAGATGGTAAAAAGAAGAAAAAGAAGTCAAAGACAAAGTGTGTAATTATGTAGA-3′ and antisense nucleotide 5′-GATCTCTACATAATTACACACTTTGTCTTTGACTTCTTTTTTCTTCTTTTTACCATCTTTGCTCATCTTG-3′ into BamHI of pEGFP-C1. pcDNAI-$G\alpha_q$-GFP, pcDNAI-$G\beta_1$, and pcDNAI-$G\gamma_2$ were gifts of C. A. Berlot (Weis Center for Research) (15). pcDNA3-HA-$G\alpha_q$, -HA-$G\alpha_s$, and -EE-$G\alpha_{i2}$ were provided by P. B. Wedegaertner (Thomas Jefferson University) (8). The Lck cDNA was provided by A. Weiss (University of California, San Francisco) and was subcloned into pcDNA3.1. pcDNA3-$G\alpha_s$-GFP and cDNA of mCherry were provided by M. M. Rasenick (University of Illinois at Chicago) (39) and R. Y. Tsien (University of California, San Diego) (31), respectively.

siRNAs. All siRNAs were purchased from Qiagen (Vento, Netherlands): DHHC3, validated Hs_ZDHHC3_5_HP, and AllStars negative control siRNA. For human DHHC7, DHHC9, $G\alpha_q$, and $G\alpha_{11}$ knockdown, the following target sequences were used: DHHC7, AGGAAACGCTACGAAAGAATA; DHHC9, ATCGTCTATGTGGCCCTCAAA; $G\alpha_q$, CAGGACACATCGTTCGATTTA and CAGGAATGCTATGATAGACGA; and $G\alpha_{11}$, CCCGGGCATCCAGGAATGCTA and CCGCATCGCCACCTTGGGCTA.

Quantitative PCR. Total RNA was extracted using TRIzol (Invitrogen), and cDNA was synthesized using a high-capacity cDNA RT kit (Applied Biosciences). Quantitative PCR was performed using an Applied Biosystems 7000 system (Applied Biosciences) and Power SYBR green PCR Master Mix (Applied Biosciences). Primers were the following: DHHC3, 5′-CTGTGCCATCGTTACCTGGTTTC-3′ and 5′-CTGCCCAGGCTTCAACTGTAAAC-3′; DHHC7, 5′-TGCAGACTTCGTGGTGACTTTCG-3′ and 5′-TGGGGCACTTGTAGATGACTTCC-3′; DHHC9, 5′-TATTTGCTGCCATGCTCTTC-3′ and 5′-GGAATCACTCCAGGGTCACT-3′; and glyceraldehyde-3-phosphate dehydrogenase (GAPDH), 5′-GTATCGTGGAAGGACTCATGACC-3′ and 5′-GTTTTCTAGACGGCAGGTCAGG-3′.

Metabolic labeling and pulse-chase assay. For pulse-chase analysis, HeLa cells (5×10^5 per six-well plate) were preincubated with 1 ml of serum-, cysteine-, and methionine-free Dulbecco's modified Eagle's medium containing 5 mg/ml fatty acid-free bovine serum albumin for 30 min. The cells were then metabolically labeled for 4 h with a medium containing 50 μCi/ml [^{35}S]methionine-cysteine (GE Healthcare) or 0.5 mCi/ml [^{3}H]palmitate (Perkin Elmer). Cells were washed and incubated in Dulbecco's modified Eagle's medium containing 100 μM palmitate. At indicated time points (see Fig. 1E), labeled cells were subjected to anti-$G\alpha_{q/11}$ immunoprecipitation (IP). Briefly, labeled cells were lysed with 100 μl of 1% sodium dodecyl sulfate (SDS)-containing IP buffer (50 mM Tris-HCl [pH 7.5], 100 mM NaCl, 1 mM EDTA, 1% Triton X-100, and 50 μg/ml phenylmethylsulfonyl fluoride). After a 5-min extraction, 900 μl of SDS-free IP buffer was added. After centrifugation at $10{,}000 \times g$ for 10 min, the supernatants were incubated with 2 μg of antibody for 1 h and then incubated with 30 μl of protein A-Sepharose (GE Healthcare). The immunoprecipitates were separated by SDS-polyacrylamide gel electrophoresis (PAGE). Gels were silver stained (Daiichi) for ^{35}S detection or treated with Amplify (GE Healthcare) for ^{3}H detection. Dried gels were exposed to films at −80°C.

Screening of the candidate PATs was performed in HEK293T cells as described previously (11, 12). To detect palmitoylation of endogenous $G\alpha_{q/11}$ in siRNA-treated cells, cells were metabolically labeled with 0.5 mCi/ml [^{3}H]palmitate-containing medium for 4 h at 72 h after siRNA transfection. Cells were then lysed and subjected to anti-$G\alpha_{q/11}$ IP, followed by fluorography. For hydroxylamine treatment, [^{3}H]palmitate-labeled cells were collected and sonicated in phosphate-buffered saline and then mixed with an equal volume of 1 M hydroxylamine (NH_2OH) (pH 7.0) or 1 M Tris-HCl (pH 7.0). After a 1-h incubation at room temperature, the cell lysates were subjected to fluorography and Western blotting.

In vitro PAT assay. The PAT assay (final volume, 50 μl) was performed as described previously, with modification (11). $G\alpha_q$-GFP and FLAG-DHHC3 were immunoprecipitated from transfected HEK293T cells using anti-GFP antibody and protein A-Sepharose and M2 anti-FLAG agarose beads (Sigma), respectively. Eluted FLAG-DHHC3 (50 nM) was added to $G\alpha_q$-GFP (50 nM) immobilized beads in 24 mM morpholineethanesulfonic acid (pH 6.4), 8 mM Tris-HCl (pH 7.5), and 0.008% Triton X-100. The reaction was started by the addition of 0.5 μM [^{3}H]palmitoyl-coenzyme A (CoA; 0.5 μCi) and incubated for 10 min at 30°C. The reaction was stopped by the addition of IP buffer and washed three times with ice-cold IP buffer. Then, the $G\alpha_q$-GFP-containing beads were suspended in SDS sample buffer with 10 mM dithiothreitol. Samples were then resolved by SDS-PAGE, followed by fluorography and Western blotting.

Immunofluorescence analysis. HeLa cells were seeded onto poly-D-lysine (10 μg/ml)-coated 12-mm glass slips (Fisher brand). Cells were fixed with 4% paraformaldehyde, 120 mM sucrose, and 100 mM HEPES (pH 7.4) for 10 min and permeabilized with 0.1% Triton X-100 for 10 min. For $G\alpha_{q/11}$ staining, the cells were fixed with methanol for 5 min at −20°C. Cells were then stained with indicated antibodies. Fluorescent images were obtained using an LSM5 Exciter system (Carl Zeiss) with a Plan-Apochromat 63× objective.

Rescue experiment. HeLa cells (4×10^3) were seeded onto poly-D-lysine-coated 12-mm glass slips. Cells on a slip were transfected with 10 pmol of siRNA and 10 ng of siDHHC3 (siRNA targeting DHHC3)-resistant GFP-mDHHC3 expression vector in 24-well plates. At 72 h after transfection, cells were fixed with 4% paraformaldehyde, permeabilized, and stained with antibodies to GFP,

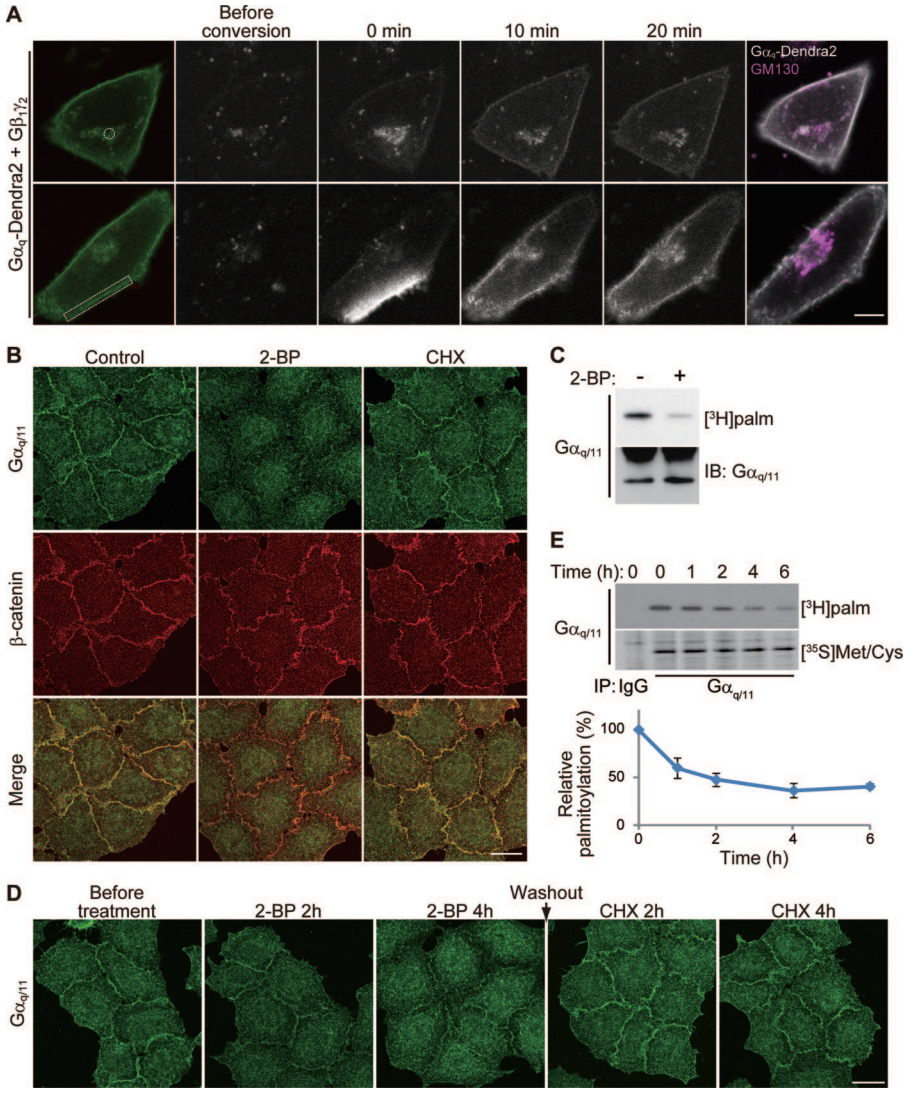

FIG. 1. Dynamic palmitate turnover on $G\alpha_{q/11}$. (A) $G\alpha_q$ shuttles between the PM and the Golgi apparatus. When $G\alpha_q$-Dendra2, $G\beta_1$, and $G\gamma_2$ were coexpressed in HeLa cells, $G\alpha_q$-Dendra2 (green) was localized at the PM and the endomembrane. $G\alpha_q$-Dendra2 in the endomembranes (upper) and a part of PM (lower) within the white regions was photoconverted by 405-nm laser. Converted $G\alpha_q$-Dendra2 (gray scale) was monitored for 20 min. Cells were then immunostained with anti-GM130 (magenta) antibody (right). Scale bar, 10 μm. (B) Inhibition of palmitoylation causes detachment of $G\alpha_{q/11}$ from the PM. HeLa cells were treated with 2-BP (100 μM) or CHX (20 μg/ml) for 4 h. The cells were then doubly stained with anti-$G\alpha_{q/11}$ (green) and anti-β-catenin (red) antibodies. Scale bar, 20 μm. (C) 2-BP blocks palmitoylation of $G\alpha_{q/11}$. HeLa cells were metabolically labeled with [^{3}H]palmitate ([^{3}H]palm) for 4 h either in the presence or absence of 2-BP. $G\alpha_{q/11}$ was immunoisolated and subjected to fluorography (upper) or Western blotting (lower). IB, immunoblotting. (D) HeLa cells were treated with 2-BP for 4 h. Then, 2-BP was washed out, and protein synthesis was inhibited by 20 μg/ml CHX for 4 h. The cells were stained with anti-$G\alpha_{q/11}$ antibody at the indicated times. The inhibition of palmitoylation for 4 h caused delocalization of $G\alpha_{q/11}$ from the PM. The $G\alpha_{q/11}$ dispersed by 2-BP came back to the PM again within 2 h after removal of 2-BP in the presence of CHX, indicating that the relocalization of $G\alpha_{q/11}$ depends on palmitoylation and depalmitoylation. Scale bar, 20 μm. (E) Pulse-chase analysis of $G\alpha_{q/11}$ palmitoylation. HeLa cells were labeled with [^{3}H]palmitate or [^{35}S]methionine-cysteine ([^{35}S]Met/Cys) for 4 h. After incubation with chase medium for 0, 1, 2, 4, and 6 h, cells were lysed and subjected to IP with anti-$G\alpha_{q/11}$ antibody. Immunoprecipitates were separated by SDS-PAGE, followed by fluorography. The ratio of [^{3}H]palmitate to [^{35}S]methionine-cysteine -labeled $G\alpha_{q/11}$ was plotted in the graph. Error bars show ±SD (n = 3). IgG, control immunoglobulin G.

$G\alpha_{q/11}$, and β-catenin. Because overexpressed DHHC3 sometimes mislocalizes substrate proteins at the Golgi apparatus, we limited the amount of plasmid to mildly express DHHC3. To quantitate the intensity of $G\alpha_{q/11}$ at the PM and the cytosol, 20 GFP-DHHC3-expressing cells were randomly chosen. The regions of the PM and cytosol were traced by polyline drawing, and their mean intensities were measured using Zeiss ZEN software. The relative PM intensities were calculated by the ratio of mean intensities of the PM and cytoplasmic regions.

Living-cell imaging. HeLa cells were seeded onto a poly-D-lysine-coated 35-mm glass-bottom dish (Iwaki) and observed at 37°C in a CO_2 chamber (Tokai Hit). For photoconversion analysis, $G\alpha_q$-Dendra2 at the Golgi apparatus or PM was converted with a 405-nm laser using an LSM5 Exciter system and Zeiss ZEN software. Images were obtained every 5 min. After live imaging, the cells were fixed and stained by anti-GM130 antibody. For fluorescence recovery after photobleaching (FRAP) analysis, $G\alpha_q$-GFP at the GalT-mCherry-positive region was bleached with a 488-nm laser. Images were acquired every 10 s for 20 min with or without 2-BP, and the average intensities of the regions were plotted in the graph. Microscope control and all image analysis were performed with Carl Zeiss ZEN software. For total internal reflection fluorescence microscopy

(TIRFM) imaging, transfected HeLa cells were observed at 37°C by an IX81 TIRF system (Olympus) with a Plan-Apochromat 100× TIRFM objective. Images were captured using an ImageEM charge-coupled-device camera (C9100-13; Hamamatsu). Fluorescent intensities from epifluorescence and TIRF images were analyzed using MetaMorph software (version 7.1; MDS Analytical Technologies).

α_{1A}-AR-dependent CREB phosphorylation. HeLa cells (1.5×10^5) in a 12-well plate were transfected with α_{1A}-AR. At 24 h after transfection, cells were stimulated with 50 μM phenylephrine with or without prazosin for 5 min. Cells were then lysed with IP buffer, and proteins were precipitated by addition of 1/10 volume of 100% trichloroacetic acid. Pellets were rinsed with acetone three times, suspended in 200 μl of SDS sample buffer, and subjected to anti-CREB or anti-phospho-CREB (pCREB) immunoblotting. For $G\alpha_{q/11}$ rescue experiments, siRNA-transfected cells were reseeded at 30 h after transfection and subjected to the second-round transfection of $G\alpha_q$-HA and α_{1A}-AR expression plasmids at 48 h after siRNA transfection. At 72 h after siRNA transfection, cells were stimulated with phenylephrine for 5 min. For DHHC3/DHHC7 knockdown experiments, cells were transfected with siRNA and α_{1A}-AR, and stimulated with phenylephrine at 72 h after transfection.

For pCREB immunostaining of DHHC knockdown cells, HeLa cells were cotransfected with siRNA and a limited amount of GFP-DHHC3 expression vector as described in the paragraph "Rescue experiment" above. At 72 h after transfection, cells were stimulated with phenylephrine and fixed with 4% paraformaldehyde, permeabilized, and stained with anti-pCREB antibody.

Measurement of IP_3 production. HeLa cells (3×10^5) expressing α_{1A}-AR were stimulated with phenylephrine (50 μM) for 10 min. Inositol triphosphate (IP_3) was extracted from the cells by incubation with 1.7% $HClO_4$ for 20 min on ice. Quantification of IP_3 was performed using an IP_3 ^3H biotrak assay system (GE Healthcare), which is based on competition between [^3H]IP_3 (the tracer) and unlabeled IP_3 in samples for binding to an IP_3-binding protein prepared from bovine adrenal cortex.

Statistical analysis. The results are expressed as mean ± standard deviation (SD). Statistical comparisons between groups were done by a Student *t* test.

RESULTS

Dynamic palmitate cycling on $G\alpha_q$. Taking advantage of $G\alpha_q$ tagged with Dendra2, a green-to-red photoconvertible fluorescent protein, we first visualized the dynamic movement of $G\alpha_q$ in HeLa cells. When $G\alpha_q$-Dendra2 was coexpressed with $G\beta_1$ and $G\gamma_2$ subunits in HeLa cells, $G\alpha_q$-Dendra2 was localized at the PM and weakly distributed in the endomembranes (Fig. 1A). Photoconverted $G\alpha_q$-Dendra2 in the endomembranes was rapidly targeted to the PM within 10 min (Fig. 1A, upper panel). In contrast, photoconverted $G\alpha_q$-Dendra2 in the PM region diffused throughout the PM, and some population of $G\alpha_q$-Dendra2 accumulated in the GM130-labeled endomembranes (i.e., Golgi apparatus) in a retrograde manner (Fig. 1A, lower panel). These results indicate that $G\alpha_q$ dynamically shuttles between the PM and the Golgi apparatus. Consistently, similar shuttling between the PM and endomembranes was recently observed by H-Ras/N-Ras-GFP (27) and $G\alpha_o$-GFP (2).

A previous study using GFP-tagged $G\alpha_q$ showed that palmitoylation of $G\alpha_q$ is essential for its membrane targeting (15). We examined whether palmitoylation of $G\alpha_q$ is a dynamic process in HeLa cells. Because the antibody against $G\alpha_q$ cross-reacts with $G\alpha_{11}$, the closest isoform (90% identity), we describe them as $G\alpha_{q/11}$. Treatment of the HeLa cells for 4 h with 2-BP, an inhibitor of protein palmitoylation, relocalized $G\alpha_{q/11}$ from the PM at the cell-to-cell contact sites to the cytoplasm (Fig. 1B) and blocked palmitoylation of $G\alpha_{q/11}$ (Fig. 1C). This treatment did not affect the PM localization of β-catenin, a component of adherence junction used as a control. The effect of 2-BP on $G\alpha_{q/11}$ localization is not simply due to disrupting palmitoylation of newly synthesized $G\alpha_{q/11}$ because CHX, an inhibitor of protein synthesis, did not affect the $G\alpha_{q/11}$ localization at the PM (Fig. 1B). $G\alpha_{q/11}$ dispersed by 2-BP came back to the PM again within 2 h after removal of 2-BP in the presence of CHX (Fig. 1D). Furthermore, the pulse-chase experiments with [^3H]palmitate and [^{35}S]methionine-cysteine revealed that palmitate on $G\alpha_{q/11}$ turns over rapidly (Fig. 1E). The half-life of palmitate on $G\alpha_{q/11}$ is approximately 2 h, whereas the half-life of $G\alpha_{q/11}$ protein itself is much longer, about 35 h. These results suggest that the de-/repalmitoylation cycle on $G\alpha_q$ dynamically regulates $G\alpha_q$ subcellular localization.

Screening of Gα palmitoylating enzymes. To understand the molecular mechanisms for dynamic regulation of $G\alpha_q$ localization, we screened the candidate $G\alpha_q$-palmitoylating enzyme. We transfected individually 23 DHHC proteins (11) together with $G\alpha_q$-GFP in HEK293T cells and assessed palmitoylation of $G\alpha_q$-GFP by metabolic labeling with [^3H]palmitate (Fig. 2A). Only DHHC3/GODZ and DHHC7/SERZ-β showed robust PAT activity toward $G\alpha_q$. Western blotting with anti-HA antibody indicates that all transfected HA-DHHC clones express in HEK293T cells albeit at different levels. Because some DHHC proteins, such as DHHC16, -20, and especially -21 express at much lower levels than DHHC3 and -7, it is possible that the clones with lower levels of expression have PAT activity toward $G\alpha_q$. To verify the possibility, we limited the amount of transfected DHHC3 and examined the PAT activity. The limited DHHC3, even at a 1:50 transfection ratio, still induced $G\alpha_q$ palmitoylation (Fig. 2B). Under these conditions, DHHC proteins except for DHHC21 were expressed at higher (or equivalent) levels than limited DHHC3 and showed no PAT activity toward $G\alpha_q$ (Fig. 2B). DHHC21 apparently showed the PAT activity toward Lck in spite of a very low expression level, whereas DHHC3 did not show activity toward Lck (Fig. 2C). These results indicate that the expression level of DHHC clones hardly affects our screening results.

$G\alpha_q$ palmitoylation induced by DHHC3 and -7 is mediated by a labile thioester bond because the [^3H]palmitate incorporated into $G\alpha_q$ was released with 0.5 M hydroxylamine treatment (Fig. 2D). We also found that the DHHC motif in DHHC3 and -7 was essential for $G\alpha_q$ palmitoylation because mutating a cysteine residue in the DHHC motif to serine in DHHC3 and -7 blocked their effects on $G\alpha_q$ palmitoylation (Fig. 2E). Furthermore, palmitoylation by DHHC3 and -7 required cysteines 9 and 10 of $G\alpha_q$ (Fig. 2E).

We next investigated whether other Gα subunits such as $G\alpha_s$ and $G\alpha_{i2}$ are also palmitoylated by DHHC3 and -7. We systematically screened candidate PATs for $G\alpha_s$ and $G\alpha_{i2}$ (data not shown) and found that DHHC proteins showed similar specificity for palmitoylation of $G\alpha_s$ and $G\alpha_q$ (Fig. 2F). However, $G\alpha_{i2}$, which undergoes both myristoylation and palmitoylation, was palmitoylated by DHHC3 and -7 and, to a lesser extent, by DHHC2 and DHHC21 (Fig. 2F). Thus, DHHC3 and -7 are common candidate PATs for $G\alpha_q$, $G\alpha_s$, and $G\alpha_{i2}$. We noted that DHHC3 and -7 show high conservation (87% identity) in the catalytic DHHC domain and form a subfamily in the phylogenetic tree of DHHC proteins (9, 11).

We next asked whether purified DHHC3 and -7 could directly palmitoylate purified $G\alpha_q$ in vitro. We immunoisolated FLAG-DHHC3 and $G\alpha_q$-GFP from transfected HEK293T

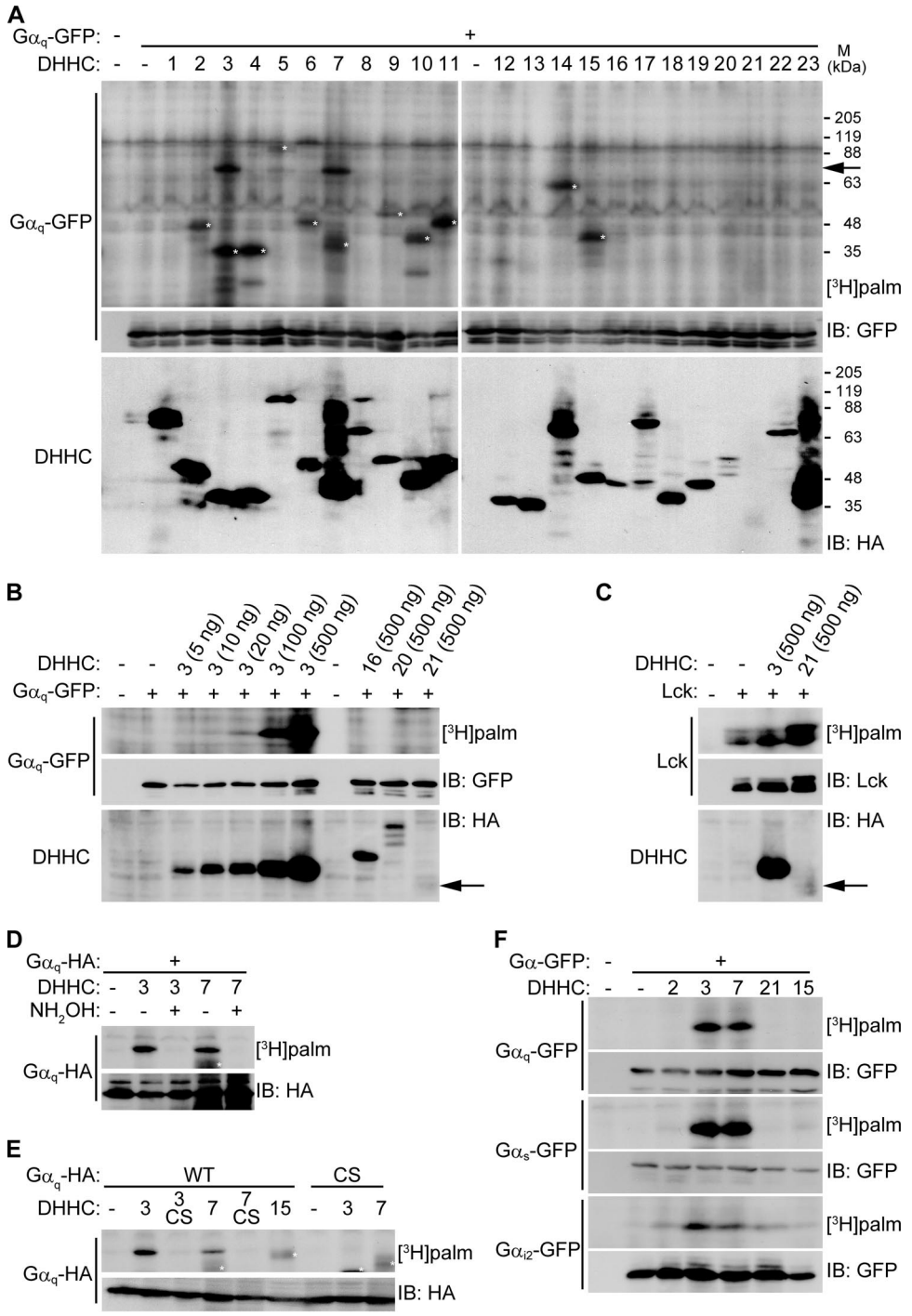

FIG. 2. Screening of potential $G\alpha_q$ palmitoylating enzymes. (A) Individual HA-DHHC clones (0.5 μg plasmid) were transfected with $G\alpha_q$-GFP (0.5 μg) into HEK293T cells. After metabolic labeling with [^{3}H]palmitate, proteins were separated by SDS-PAGE, followed by fluorography and Western blotting with anti-GFP antibody for $G\alpha_q$-GFP and anti-HA antibody for DHHC proteins. An arrow indicates the position of $G\alpha_q$-GFP. White asterisks indicate autopalmitoylation of expressed DHHC proteins. Coexpression of DHHC3 or -7 robustly and specifically increased $G\alpha_q$ palmitoylation. Note that several DHHC proteins, such as DHHC16, -20, and -21, express at lower levels than DHHC3 and -7. M, molecular mass. (B) HEK293T cells were transfected with the indicated amount of DHHC proteins with $G\alpha_q$-GFP and were labeled with [^{3}H]palmitate. DHHC16 and -20 did not increase $G\alpha_q$ palmitoylation, whereas limited DHHC3 expression by 10 ng of plasmids (showing expression levels similar to DHHC16 and -20) still enhanced $G\alpha_q$ palmitoylation. An arrow indicates the position of DHHC21. (C) Although DHHC21 expressed at a lower level than DHHC3, DHHC21 has apparent PAT activity toward Lck. An arrow indicates the position of DHHC21. (D) Treatment of labeled cell lysates with 0.5 M hydroxylamine (NH_2OH) but not 0.5 M Tris-HCl (−) released DHHC3- or DHHC7-mediated [^{3}H]palmitate incorporated into $G\alpha_q$-HA, indicating that DHHC3- or DHHC7-induced palmitoylation is mediated by a thioester bond. (E) The DHHC3(C157S) and DHHC7(C160S) mutations (shown as CS) abolished the palmitoylating activity. The mutations cysteines 9 and 10 in $G\alpha_q$ (CS) abolished its palmitoylation. Asterisks indicate the autopalmitoylation of DHHCs. (F) HEK293T cells cotransfected with indicated DHHC clones (2, 3, 7, 21, and 15) and Gα-GFP subfamily (α_q, α_s, and α_{i2}) were metabolically labeled with [^{3}H]palmitate. All Gα members were palmitoylated by DHHC3 and DHHC7. $G\alpha_{i2}$ was also palmitoylated by DHHC2 and DHHC21 to a lesser extent. WT, wild type; IB, immunoblotting.

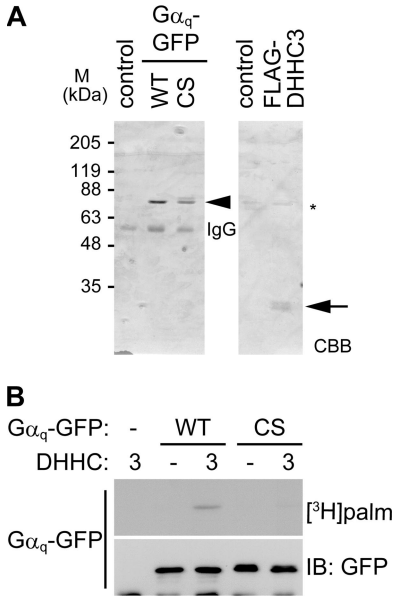

FIG. 3. DHHC3 directly palmitoylates $G\alpha_q$ in vitro. (A) Immunopurified GFP-tagged wild-type (WT) $G\alpha_q$ and $G\alpha_q$ (CS) and FLAG-DHHC3 were stained with Coomassie brilliant blue (CBB). An arrowhead and an arrow indicate the positions of $G\alpha_q$-GFP and FLAG-DHHC3, respectively. An asterisk indicates the nonspecific band. M, molecular mass. (B) Purified $G\alpha_q$ and DHHC3 were incubated in the presence of [^{3}H]palmitoyl-CoA for 10 min at 30°C. Then, radiolabeled $G\alpha_q$-GFP was evaluated by fluorography (upper) and immunoblotting (IB) with anti-GFP antibody (lower). DHHC3 palmitoylated wild-type $G\alpha_q$ but not $G\alpha_q$ (CS).

cells (Fig. 3A) and incubated them with [^{3}H]palmitoyl-CoA. Purified DHHC3 apparently mediated incorporation of radiolabeled palmitate into wild-type $G\alpha_q$-GFP (Fig. 3B). Under these conditions, spontaneous (nonenzymatic) palmitate transfer into $G\alpha_q$-GFP was not observed (Fig. 3B). A similar result was obtained by using DHHC7 instead of DHHC3 (data not shown).

Knockdown of DHHC3 and -7 impairs $G\alpha_q$ palmitoylation and PM targeting. To determine whether DHHC3 and -7 are responsible for $G\alpha_q$ palmitoylation in cells, we knocked down DHHC3 and -7. Treatment of HeLa cells with siRNAs directed against human DHHC3 and/or human DHHC7 specifically reduced the expression of DHHC3 and/or -7 (validated by quantitative RT-PCR) (Fig. 4A). When DHHC3 and/or DHHC7 was knocked down in HEK293T cells, the incorporation of [^{3}H]palmitate into endogenous $G\alpha_{q/11}$ was markedly reduced compared to control siRNA-transfected cells (Fig. 4B). A similar result was obtained in HeLa cells (data not shown). Because palmitoylation of $G\alpha_{q/11}$ was essential for its PM localization (15) (Fig. 1B and D), we performed immunofluorescence analysis of endogenous $G\alpha_{q/11}$ in HeLa cells. Knockdown of DHHC3 and/or -7 delocalized $G\alpha_{q/11}$ from the PM to the cytoplasm, whereas the intensity of β-catenin at the cell-to-cell contact sites did not change (Fig. 4C). The mislocalization of $G\alpha_{q/11}$ to the cytoplasm by siRNAs to human DHHC3 and human DHHC7 was rescued by siDHHC3-resistant wild-type mDHHC3 (Fig. 4D). In contrast, the mislocalization of $G\alpha_{q/11}$ was not rescued by the PAT-inactive mDHHC3(C157S) (Fig. 4D). We next examined the effect of DHHC3 knockdown on the $G\alpha_{q/11}$ localization in primary hippocampal neurons, in which DHHC3 plays a more dominant role than DHHC7 (9). When DHHC3 was knocked down by vector-based RNAi, $G\alpha_{q/11}$ at the PM was significantly reduced and relocalized into the cytoplasm, whereas DHHC2 knockdown did not affect the PM localization of $G\alpha_{q/11}$ (Fig. 5).

Next, to visualize $G\alpha_q$ at the cytoplasmic face of the PM with a high signal-to-noise ratio, we used TIRFM, which excites the molecules within 100-nm of the cover glass. When $G\alpha_q$-GFP was expressed in HeLa cells, strong signals throughout the ventral surface of cells were detected by TIRFM (Fig. 6A). In contrast, the TIRFM signals of $G\alpha_q$-GFP were apparently reduced when the cells were treated with 2-BP. The intensity of the palmitoylation-deficient mutant of $G\alpha_q$, i.e., $G\alpha_q$ (CS)-GFP, was also lower than that of wild-type $G\alpha_q$-GFP, suggesting that the signals visualized by TIRFM mainly reflect the membrane-bound palmitoylated $G\alpha_q$-GFP. Supporting this, the intensity of GFP-K-Ras-CAAX (where A and X represent aliphatic and any residues, respectively), which targets to the PM by polybasic and prenylation sequences, did not change on 2-BP treatment. To examine the role of DHHC3 and/or -7 in the $G\alpha_q$ localization at the PM, we treated cells with siRNAs, observed them by TIRFM and epifluorescence microscopy, and measured the intensity ratio of TIRFM images to epifluorescence images. Knockdown of DHHC3 and/or -7 reduced significantly the intensity visualized by TIRFM (Fig. 6B). Under these conditions, GFP-K-Ras-CAAX intensity by TIRFM was not affected (Fig. 6B). Taken together, these results indicate that DHHC3 and/or -7 are authentic PATs for $G\alpha_q$ and are necessary for PM targeting of $G\alpha_q$.

DHHC3 palmitoylates $G\alpha_q$ at the Golgi apparatus and drives PM-Golgi apparatus shuttling of $G\alpha_q$. We next examined the cellular location of $G\alpha_{q/11}$ palmitoylation. We first confirmed that our anti-DHHC3 antibody is specific because two bands detected by the DHHC3 antibody completely disappeared in the knocked down cell lysate (Fig. 7A). These two bands may contain (i) splicing variants as previously reported (17); (ii) differentially modified proteins by posttranslational modifications, such as phosphorylation, glycosylation, and palmitoylation; and (iii) degradation products. Consistent with previous observations in neurons (17), when HeLa cells were stained by this specific DHHC3 antibody, DHHC3 immunoreactivity occurred only at the GM130-labeled Golgi apparatus (Fig. 7B). The staining is specific because this signal disappeared in DHHC3 knocked down cells (Fig. 7B). When mCherry-DHHC3 was coexpressed with $G\alpha_q$-GFP, some $G\alpha_q$ was colocalized with DHHC3 in the Golgi apparatus (Fig. 7C). Photoconversion analysis by Dendra2-DHHC3 showed that DHHC3 localizes stably at the Golgi apparatus (Fig. 7D), in contrast to $G\alpha_q$ (Fig. 1A). These results strongly suggest that DHHC3 palmitoylates $G\alpha_q$ at the Golgi apparatus. We also found that HA-tagged DHHC7 showed similar distribution to DHHC3 at the Golgi apparatus (data not shown).

To examine the role of DHHC3 and -7 in the dynamic shuttling of $G\alpha_q$, the $G\alpha_q$ dynamics were assessed by monitoring FRAP. To mark the Golgi apparatus, we coexpressed mCherry-tagged GalT (16, 34) together with $G\alpha_q$-GFP with or without the β_1 and γ_2 subunits. After GFP fluorescence at the Golgi apparatus was bleached, $G\alpha_q$-GFP fluorescence at the Golgi apparatus recovered within 20 min (64.6% ± 14.3%)

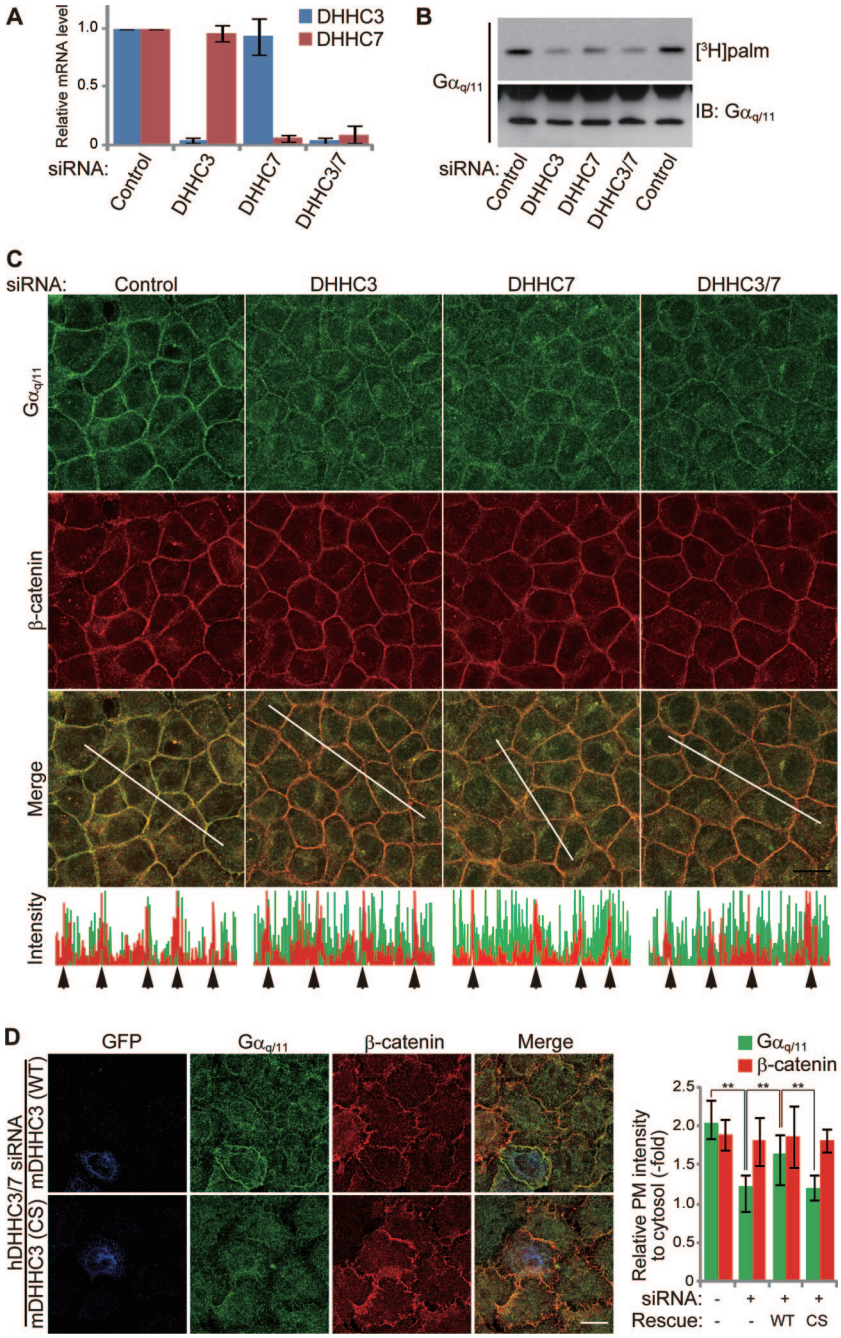

FIG. 4. DHHC3 and -7 are necessary for $G\alpha_{q/11}$ palmitoylation and PM localization. (A) DHHC3 and -7 siRNAs downregulate targeted mRNA expressions. HeLa cells were transfected with a control or DHHC3 or -7 siRNA duplex. At 72 h after transfection, the expression of DHHC3 or -7 mRNA was quantitated by real-time RT-PCR. The expression of DHHC3 and -7 was normalized to that of GAPDH. Error bars show ±SD (n = 3). (B) HEK293T cells were transfected with the indicated siRNAs, and cells were labeled with [^{3}H]palmitate for 4 h. Endogenous $G\alpha_{q/11}$ was then immunoprecipitated, followed by fluorography and Western blotting. (C) HeLa cells were transfected with the indicated siRNAs and doubly stained with anti-$G\alpha_{q/11}$ (green) and anti-β-catenin (red) antibodies. Note that knockdown of DHHC3 and/or DHHC7 specifically impairs PM localization of $G\alpha_{q/11}$. Graphs indicate fluorescent intensity along white lines. Arrows mark the cell-to-cell contact sites along the white line. Scale bar, 20 μm. (D) siRNAs to human-specific DHHC3 and DHHC7 were cotransfected into HeLa cells together with wild-type (WT) GFP-mDHHC3 or catalytically inactive GFP-mDHHC3(C157S) [mDHHC3(CS)]. Cells were immunostained with anti-GFP (blue), anti-$G\alpha_{q/11}$ (green), and anti-β-catenin (red) antibodies. The colors are pseudocolors. Scale bar, 20 μm. Relative fluorescence intensities of PM to cytosol are shown (right graph). Error bars show ±SD (n = 20). **, $P < 0.01$. IB, immunoblotting.

(Fig. 8A). This newly arrived $G\alpha_q$-GFP did not include newly synthesized $G\alpha_q$-GFP because CHX did not affect the fluorescence recovery (data not shown). Because the fluorescence recovery of $G\alpha_q$-GFP at the Golgi apparatus was not affected in the presence or absence of $\beta_1\gamma_2$ subunits (Fig. 8A), we expressed only $G\alpha_q$-GFP in the following experiments. We next asked whether palmitoylation is involved in the retrograde PM-Golgi trafficking of $G\alpha_q$-GFP. We found that inhibition of

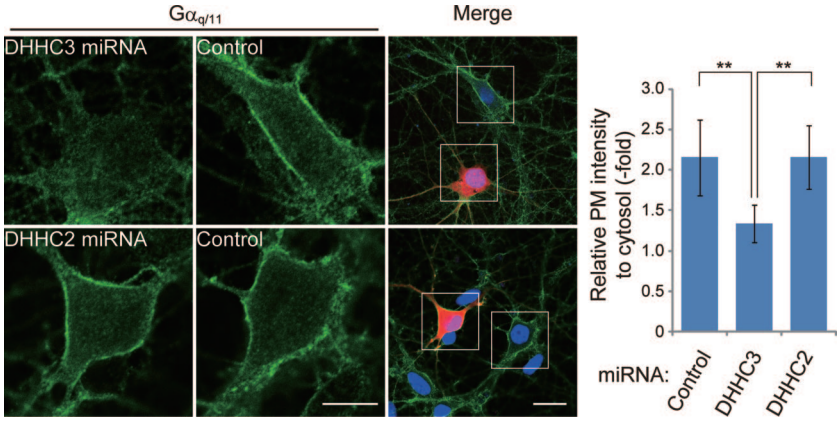

FIG. 5. Depletion of DHHC3 expression impairs the PM targeting of $G\alpha_{q/11}$ in hippocampal neurons. Rat hippocampal neurons (DIV8) were transfected with mCherry-miR RNA (to rat DHHC2 or -3) expression vectors (red). At 7 days after transfection, neurons were fixed and stained with anti-$G\alpha_{q/11}$ antibody (green) and Hoechst (blue). Scale bars, 5 μm (high magnification) and 10 μm (low magnification). Graph shows ratio of fluorescence intensities of the PM to the cytosol. Error bars show ±SD ($n = 12$). **, $P < 0.01$. miRNA, microRNA.

protein palmitoylation by 2-BP significantly reduced the fluorescence recovery at the GalT-positive Golgi region (33.3% ± 3.7%; $P < 0.05$ compared to control) (Fig. 8B), indicating that palmitoylation of $G\alpha_q$ at the Golgi apparatus is necessary for the retrograde trafficking from the PM to the Golgi apparatus. $G\alpha_q$-GFP intensity in the cytoplasm and at the PM did not apparently change during the 20-min observation with 2-BP treatment. In contrast, the apparent delocalization of endoge-

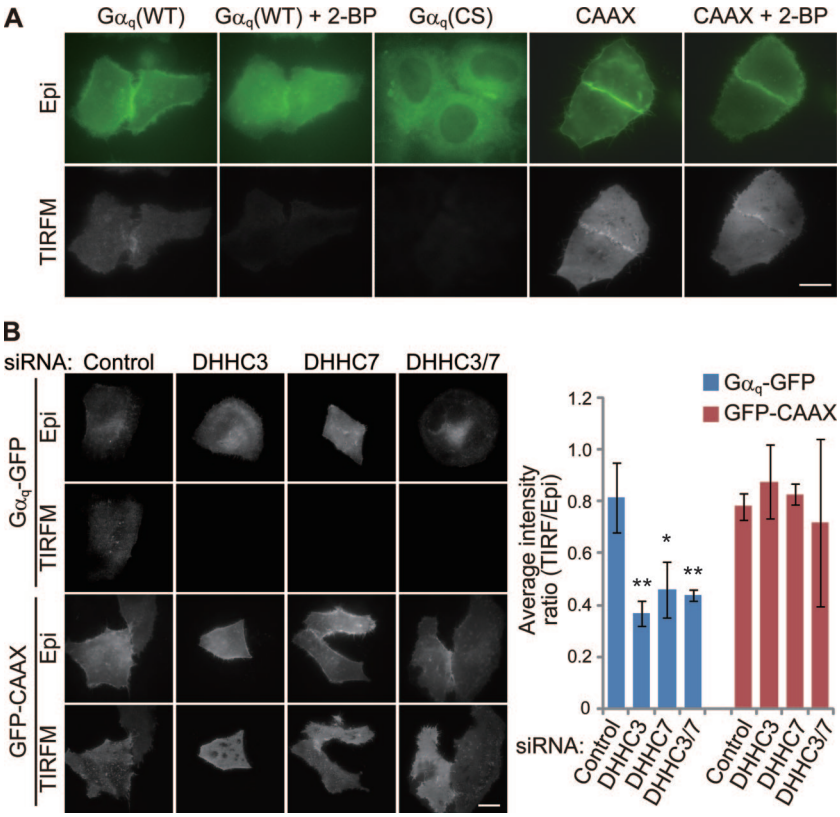

FIG. 6. TIRFM imaging of membrane-bound palmitoylated $G\alpha_q$. (A) HeLa cells were transfected with GFP-tagged $G\alpha_q$ (WT), palmitoylation-deficient $G\alpha_q$ (CS), or the C-terminal sequence of K-Ras including polybasic and prenylation sequences (GFP-CAAX). Cells were observed by epifluorescence microscopy (Epi) and TIRFM before and at 4 h after treatment with 2-BP. $G\alpha_q$-GFP was clearly detected by TIRFM, and the intensity was reduced on 2-BP treatment. The intensity of $G\alpha_q$ (CS) was apparently weaker than that of $G\alpha_q$ (WT). Scale bar, 20 μm. (B) HeLa cells were transfected with control or DHHC3/DHHC7 siRNAs together with $G\alpha_q$-GFP or GFP-CAAX. Scale bar, 20 μm. Relative fluorescence intensities of cell images from TIRFM compared to those of epifluorescence microscopy are indicated in the graph. Note that $G\alpha_q$-GFP intensity visualized by TIRFM was reduced significantly in DHHC3 and DHHC7 knocked down cells. Error bars show ±SD ($n = 5$). **, $P < 0.01$; *, $P < 0.05$.

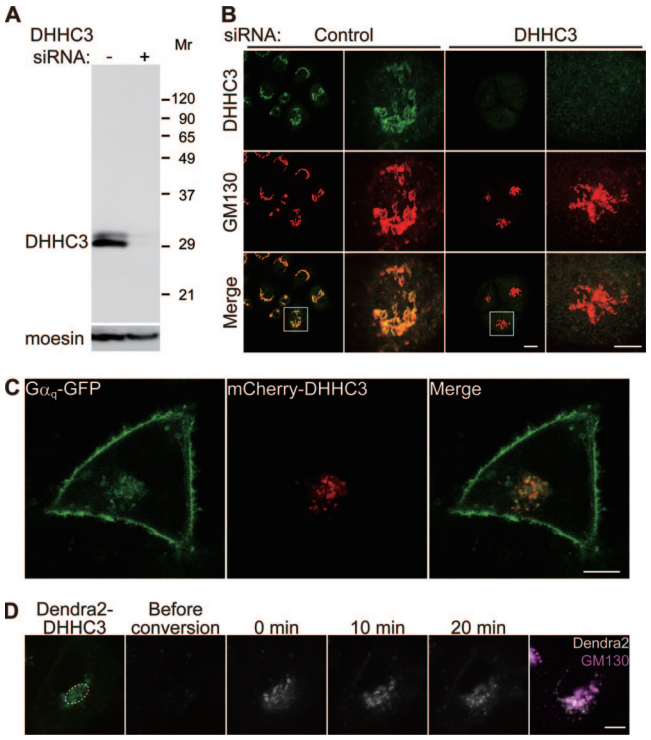

FIG. 7. $G\alpha_q$ and DHHC3 colocalize to the Golgi apparatus. (A) HeLa cells were transfected with control or DHHC3 siRNA. The lysates were then immunoblotted with anti-DHHC3 and anti-moesin antibodies, indicating that DHHC3 antibody specifically detects endogenous DHHC3. Molecular weights (in thousands) are shown at the right. (B) HeLa cells transfected with control or DHHC3 siRNA were immunostained with antibodies to DHHC3 (green) and Golgi marker GM130 (red). White boxes are magnified. The Golgi staining by DHHC3 antibody is specific because the signal disappeared in siDHHC3-treated cells. Scale bars, 20 μm (low magnification) and 10 μm (high magnification). (C) HeLa cells were cotransfected with $G\alpha_q$-GFP and mCherry-DHHC3. Some population of $G\alpha_q$ was colocalized with DHHC3 at the Golgi apparatus. Scale bar, 20 μm. (D) Dendra2-DHHC3 (green) at the Golgi apparatus was photoconverted (gray scale). DHHC3 was stably localized at the Golgi apparatus, where GM130 was labeled (magenta). Scale bar, 10 μm.

nous $G\alpha_q$ from the PM to the cytoplasm was observed at 4 h after 2-BP treatment (Fig. 1B). Judging from the half-life of palmitate on $G\alpha_q$ (about 2 h, based on Fig. 1E), these results are consistent. In fact, our longer observation confirmed that $G\alpha_q$-GFP was relocalized from the PM to the cytoplasm at 4 h after 2-BP treatment (data not shown). When DHHC3 and -7 were knocked down by siRNAs, $G\alpha_q$-GFP was apparently localized in the cytoplasm and not localized at the Golgi apparatus (Fig. 8C). The recovery of fluorescence around the GalT-positive Golgi region was rapid and nearly complete (94.6% ± 4.8%) (Fig. 8C). Palmitoylation-deficient $G\alpha_q$ (CS)-GFP showed a similar cytoplasmic distribution and rapid recovery both around the GalT-positive region (Fig. 8D, CS region 1) and at cytoplasmic regions (Fig. 8D, CS region 2). This rapid recovery is not due to the enhanced retrograde PM-Golgi trafficking but simply to free diffusion of soluble cytoplasmic proteins. Taken together with the data presented in Fig. 1A, these results indicate that $G\alpha_q$ repalmitoylation by Golgi compartment-resident DHHC3/DHHC7 is necessary for temporal trapping of $G\alpha_q$ at the Golgi apparatus, leading to the constitutive Golgi compartment-PM shuttling.

DHHC3 and -7 are involved in the GPCR-mediated signaling pathway. Next, we investigated whether DHHC3 and -7 are involved in the physiologic GPCR-mediated signal transduction. We selected α_{1A}-AR as the $G\alpha_{q/11}$-coupled receptor and monitored its downstream signaling by pCREB (28) and IP_3 production. When HeLa cells transiently transfected with α_{1A}-AR were stimulated with phenylephrine, an α_{1A}-AR agonist, the phosphorylation level of CREB increased (Fig. 9A and D). This increase was completely blocked by the coapplication of prazosin, an α_{1A}-AR antagonist (Fig. 9A). Knockdown of $G\alpha_{q/11}$ inhibited α_{1A}-AR activation-induced CREB phosphorylation (Fig. 9B), indicating that α_{1A}-AR-mediated CREB phosphorylation is mediated by $G\alpha_{q/11}$. Palmitoylation of $G\alpha_{q/11}$ is necessary for the α_{1A}-AR -mediated signaling pathway because wild-type $G\alpha_q$ (RNAi-resistant mouse $G\alpha_q$), but not the palmitoylation-deficient $G\alpha_q$ (CS), rescued α_{1A}-AR-mediated CREB phosphorylation (Fig. 9B). Furthermore, DHHC3 and -7 knockdown significantly blocked α_{1A}-AR-mediated CREB phosphorylation (Fig. 9C and D). We also found that wild-type DHHC3 (RNAi-resistant mDHHC3) but not the PAT-inactive mDHHC3(C157S), rescued α_{1A}-AR-mediated CREB phosphorylation (Fig. 9D). Finally, we examined whether DHHC3 and -7 are involved in the α_{1A}-AR/G_q-induced phospholipase C activation by measuring IP_3 production. When HeLa cells transiently transfected with α_{1A}-AR were stimulated with phenylephrine, the IP_3 production significantly increased (Fig. 9E). This increase was significantly blocked by knockdown of DHHC3 and -7 but not by knockdown of DHHC9. Thus, DHHC3 and DHHC7 play an essential role in the α_{1A}-AR-mediated GPCR signaling pathway by $G\alpha_q$ palmitoylation.

DISCUSSION

This study identified DHHC3 and DHHC7 as Gα palmitoylating enzymes that mediate palmitoyl transfer to $G\alpha_q$, $G\alpha_s$, and $G\alpha_{i2}$. Golgi compartment-resident DHHC3 and -7 play essential roles in the PM-Golgi apparatus shuttling of $G\alpha_q$. Furthermore we showed that DHHC3 and -7 are necessary for α_{1A}-AR-mediated GPCR signaling pathway through $G\alpha_q$ targeting to the PM.

Identification of Gα palmitoylating enzymes has long been controversial. Some studies have suggested that Gα palmitoylation in cells might occur nonenzymatically because the formation of palmitoyl thioester linkage on proteins could occur spontaneously in vitro in the presence of a high concentration (10 to 20 μM) of palmitoyl-CoA (4). Recent systematic proteomic analysis revealed that DHHC family proteins are the main PATs that catalyze most of the protein palmitoylation in yeast because 29 of the 30 surveyed palmitoyl proteins were not palmitoylated in yeast lacking six of seven DHHC genes (30). In addition, our systematic screening analyses using 23 mammalian DHHC clones revealed that the palmitoylation levels of the more than 20 tested substrates were all enhanced by specific DHHC proteins (9, 10, 11, 12; also data not shown). These studies strongly suggest that members of the DHHC protein family mediate Gα palmitoylation. Our analyses showed decisively that DHHC3 and -7 are authentic Gα palmitoylating

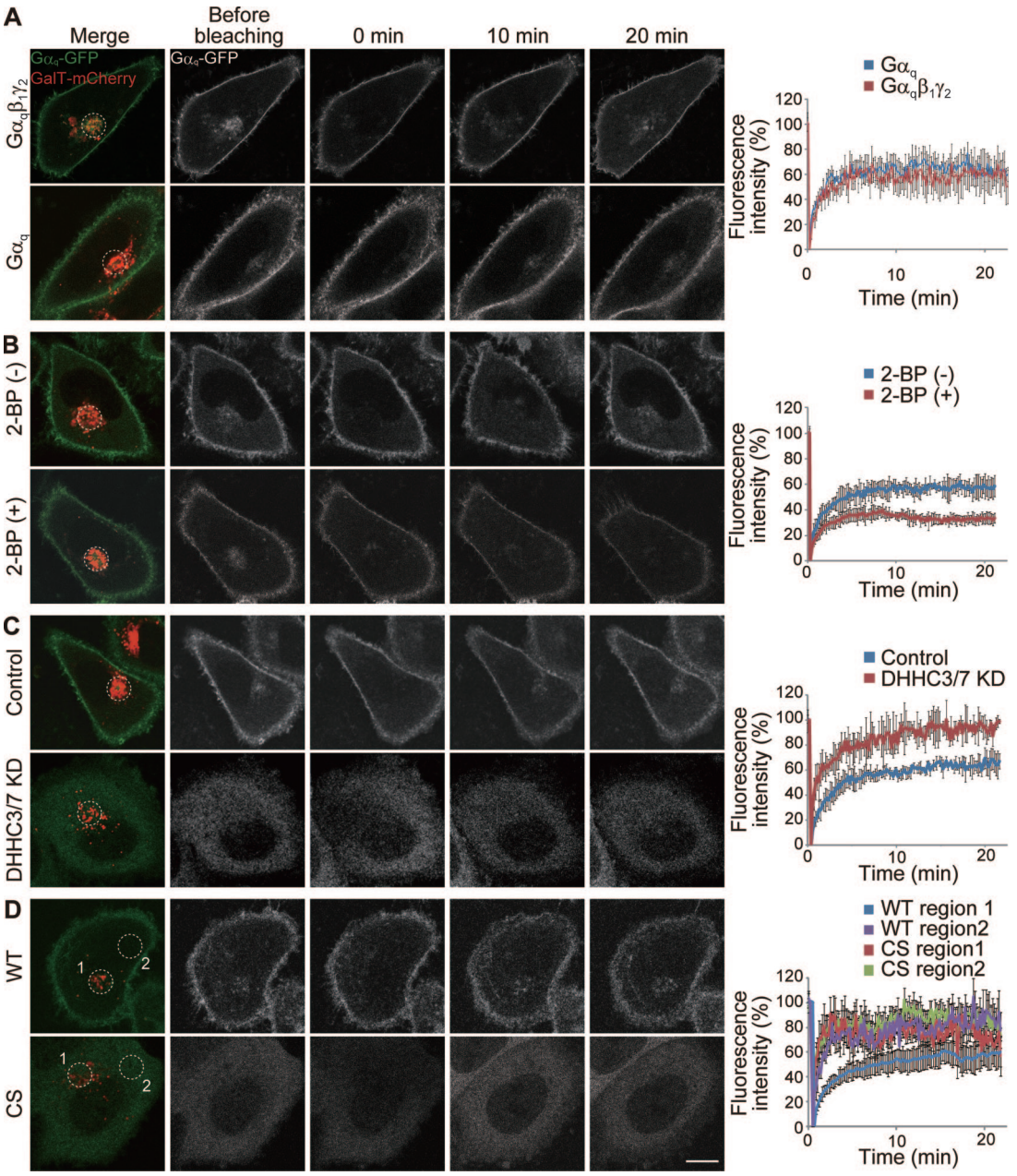

FIG. 8. Retrograde PM-Golgi trafficking of $G\alpha_q$ depends on $G\alpha_q$ palmitoylation by Golgi apparatus-resident DHHC3 and -7. (A) HeLa cells were transfected with $G\alpha_q$-GFP (green and white) and GalT-mCherry (red) expression vectors with or without $G\beta_1\gamma_2$. The Golgi region (white circle) marked by GalT-mCherry was bleached, and then fluorescent recovery of $G\alpha_q$-GFP was monitored by acquiring images every 10 s. Fluorescence intensities were plotted in graphs (right). (B) HeLa cells expressing $G\alpha_q$-GFP (green and white) and GalT-mCherry (red) were treated with or without 2-BP for 30 min before FRAP analysis. The region (white circle) identified with GalT-mCherry was bleached, and then fluorescent recovery of $G\alpha_q$-GFP was monitored. Treatment with 2-BP inhibited the recovery of fluorescence. (C) Knockdown (KD) of DHHC3 and -7 inhibited the Golgi and PM targeting of $G\alpha_q$-GFP, resulting in the diffuse cytoplasmic localization. (D) Palmitoylation-deficient $G\alpha_q$ (CS)-GFP showed similar cytoplasmic distribution and rapid recovery both around the GalT-positive region (CS region 1) and at cytoplasmic region (CS region 2). The recovery of palmitoylation deficient $G\alpha_q$ (CS)-GFP was as rapid as that of DHHC3 and -7 knocked down cells in panel C. Scale bar, 10 μm. Error bars show ±SD ($n = 5$). WT, wild type.

enzymes in vitro and in vivo. It is conceivable that similar approaches will be useful to identify PATs for other subfamilies of Gα, GPCRs, RGSs, and small GTPases.

By a knockdown approach, we found that DHHC3 and/or -7 knockdown reduces endogenous $G\alpha_q$ palmitoylation in HEK293T cells (Fig. 4B). This result raised a couple of questions. One may wonder why knockdown of DHHC3 and/or DHHC7 does not completely abolish $G\alpha_{q/11}$ palmitoylation (Fig. 4B). Because our knockdown efficiency was about 85%, judging from our immunofluorescence analysis with anti-DHHC3 antibody, the remaining $G\alpha_{q/11}$ palmitoylation may be largely derived from the nontransfected cells with siRNA or

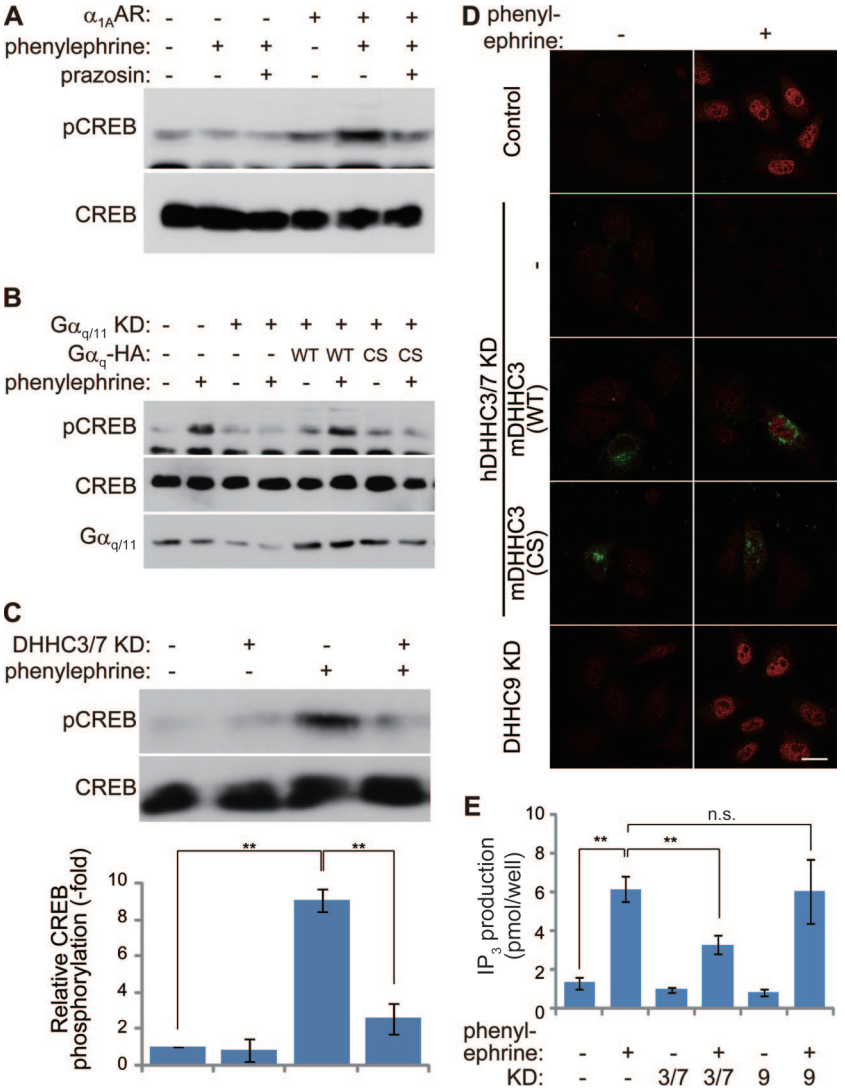

FIG. 9. DHHC3 and -7 are necessary for GPCR-mediated signal transduction through the $G\alpha_q$ palmitoylation. (A) α_{1A}-AR activation leads to CREB phosphorylation. HeLa cells transiently transfected with α_{1A}-AR were treated with 50 μM phenylephrine with or without 50 μM prazosin for 5 min. The cell lysates were treated with 10% trichloroacetic acid, and the resulting precipitates were subjected to immunoblotting with antibodies to CREB and Ser133 pCREB. (B to D) HeLa cells were transiently transfected with α_{1A}-AR and indicated plasmids or siRNAs. (B) α_{1A}-AR-mediated CREB phosphorylation requires palmitoylated $G\alpha_q$. Knockdown (KD) of $G\alpha_q$ and $G\alpha_{11}$ blocked α_{1A}-AR-induced CREB phosphorylation, and RNAi-resistant $G\alpha_q$ (WT), but not palmitoylation-deficient $G\alpha_q$ (CS), rescued α_{1A}-AR-mediated CREB phosphorylation. (C) Knocked down DHHC3 and DHHC7 (DHHC3/7 KD) inhibited α_{1A}-AR-induced CREB phosphorylation, indicating that DHHC3 and -7 are essential for the GPCR-signaling pathway through $G\alpha_q$ palmitoylation. pCREB/CREB ratios are indicated in the graph. Error bars show ±SD (n = 3). **, $P < 0.01$. (D) HeLa cells expressing α_{1A}-AR were treated with phenylephrine and stained with anti-pCREB antibody (red). Note that α_{1A}-AR stimulation induced robust phosphorylation of CREB in the nucleus. The defect of CREB phosphorylation by knocked down human DHHC3 and human DHHC7 (hDHHC3/7 KD) was rescued by GFP-mDHHC3 (WT; green) but not catalytically inactive GFP-mDHHC3 (C157S) [mDHHC3 (CS)]. Scale bar, 20 μm. (E) The HeLa cells cotransfected with α_{1A}-AR and the indicated siRNAs were treated with phenylephrine for 10 min, followed by IP_3 extraction. Average IP_3 production of three independent experiments is indicated in the graph. Agonist-induced IP_3 production was specifically blocked by knockdown of DHHC3 and -7 (KD 3/7), indicating that DHHC3 and -7 are necessary for the α_{1A}-AR-mediated GPCR signaling pathway. Error bars show ±SD (n = 3). **, $P < 0.01$; n.s., not significant ($P = 0.20$).

the cells in which DHHC3 and/or DHHC7 were partially knocked down. Although the existence of other PATs and nonenzymatic mechanisms (4) cannot be completely ruled out, our results strongly suggest that DHHC3 and DHHC7 represent major $G\alpha_{q/11}$ palmitoylating enzymes. Double-knockout experiments of DHHC3 and DHHC7 will decisively demonstrate this issue. On the other hand, others may ask why knockdown of either DHHC3 or DHHC7 reduces $G\alpha_q$ palmitoylation (Fig. 4B) although the redundancy of DHHC3 and DHHC7 is expected. A straightforward possibility is that the total amount of DHHC3 and DHHC7 limits the palmitoylation of $G\alpha_q$ in the intact cells. Acute knockdown of DHHC3 or DHHC7 may not be fully compensated by the rest of DHHC. Alternatively, DHHC3 and DHHC7 may have synergistic effects on their PAT activity. In fact, DHHC3 and DHHC7 form homo-/heteromultimers (9). Further studies using the

DHHC3/DHHC7 knockout cells/animals will be required to reveal the molecular redundancy issue.

In this study, we found that $G\alpha_q$-GFP shuttles between the PM and Golgi apparatus within 10 min in HeLa cells. In contrast, Chisari and coworkers have recently shown that $G\alpha_o$-GFP and also the β_9-γ_3 subunits cycle in a matter of seconds in CHO cells (2). These differences may depend on the cellular context. In CHO cells, the distance between the PM and the endomembrane looks much shorter than that in HeLa cells. Alternatively, the difference in acylation types of $G\alpha_q$ (dual palmitoylation) and $G\alpha_o$ (myristoylation and adjacent palmitoylation) may contribute to individual kinetics of shuttling. Because 16-carbon palmitate has higher membrane affinity than the 14-carbon myristate, dually palmitoylated $G\alpha_q$ may be more pronounced in PM localization than myristoylated/monopalmitoylated $G\alpha_o$, leading to slower retrograde trafficking. In support of this idea, Rocks and colleagues reported that monopalmitoylated N-Ras displays a faster retrograde PM-Golgi apparatus trafficking than dually palmitoylated H-Ras (27). Direct comparison between $G\alpha_q$ and $G\alpha_o$ in the same cell type will address this question.

Wedegaertner and Bourne reported that activation of β-AR accelerates the palmitate cycling on $G\alpha_s$ (depalmitoylation and subsequent repalmitoylation of $G\alpha_s$) and induces PM-to-cytosol translocation of $G\alpha_s$ (37). In contrast, another report showed that $G\alpha_q$-GFP at the PM did not change on α_{2A}-AR agonist stimulation in HEK293T cells (15). Our analysis in HeLa cells using FRAP and photoconversion methods showed that $G\alpha_q$ constitutively cycles between the PM and Golgi apparatus and that this cycling requires the palmitoylation of $G\alpha_q$ by Golgi apparatus-resident DHHC3 and -7. Although we attempted to decipher whether α_{1A}-AR agonist stimulation affects Gα dynamic relocalization, our imaging resolution could not detect a significant difference (data not shown). These results imply that Gα dynamics depend on the subfamily of Gα and cellular/agonist contexts. Considering that H-Ras and N-Ras shuttle between the PM and Golgi apparatus through de-/repalmitoylation (27), such a constitutive cycling between the PM and intracellular organelles may be a general mechanism that allows cells to rapidly adjust to extracellular stimulation. To understand the whole picture of this shuttling mechanism, examination of the effect of acyl-protein thioesterase (5), a potential depalmitoylating enzyme, or identification of a novel depalmitoylating enzyme family still needs to be done.

We investigated whether DHHC3 and -7 activity is regulated by extracellular stimulation. We found that incorporation of [^{3}H]palmitate into $G\alpha_q$ did not change when the cells were treated with an α_{1A}-AR agonist (data not shown). Also, the localization of DHHC3 at the Golgi apparatus did not change with an α_{1A}-AR agonist (data not shown). In contrast, DHHC21, one of the endothelial NO synthase PATs, was shown to be involved in the release of nitric oxide stimulated by both ionomycin and ATP, suggesting that DHHC21 is regulated downstream of calcium and ATP (10). These results imply that the individual DHHC proteins are regulated differently. Because protein palmitoylation modifies a wide variety of GPCR-related proteins and because GPCR signaling pathways play important roles in physiologic and pathological phenomena, the DHHC enzyme family may become an ideal therapeutic target.

ACKNOWLEDGMENTS

We thank K. Kaibuchi (Nagoya University), S. Kobayashi (NIBB), T. Tabira, and K. Takahashi (NCGG) for sharing equipment; T. Watanabe (Nagoya University), S. Ishii (Tokyo University), and A. Dimitrov (Institut Curie) for valuable suggestions; and D. S. Bredt (Eli Lilly and Company), C. A. Berlot (Weis Center for Research), P. B. Wedegaertner (Thomas Jefferson University), A. Weiss (University of California, San Francisco), M. M. Rasenick (University of Illinois at Chicago), and R. Y. Tsien (University of California, San Diego) for providing plasmid vectors.

R.T. and J.N. are supported by the Japan Society for the Promotion of Science. Y.F. is supported by grants from the Human Frontier Science Program (HFSP-CDA) and MEXT (18700376). M.F. and F.P. are supported by grants from HFSP (Young Investigators). M.F. is supported by grants from MEXT (20670005, 20022043, 20054022, and 18687008).

REFERENCES

1. **Bartels, D. J., D. A. Mitchell, X. Dong, and R. J. Deschenes.** 1999. Erf2, a novel gene product that affects the localization and palmitoylation of Ras2 in *Saccharomyces cerevisiae*. Mol. Cell. Biol. **19:**6775–6787.
2. **Chisari, M., D. K. Saini, V. Kalyanaraman, and N. Gautam.** 2007. Shuttling of G protein subunits between the plasma membrane and intracellular membranes. J. Biol. Chem. **282:**24092–24098.
3. **Drenan, R. M., C. A. Doupnik, M. P. Boyle, L. J. Muglia, J. E. Huettner, M. E. Linder, and K. J. Blumer.** 2005. Palmitoylation regulates plasma membrane-nuclear shuttling of R7BP, a novel membrane anchor for the RGS7 family. J. Cell Biol. **169:**623–633.
4. **Duncan, J. A., and A. G. Gilman.** 1996. Autoacylation of G protein α subunits. J. Biol. Chem. **271:**23594–23600.
5. **Duncan, J. A., and A. G. Gilman.** 1998. A cytoplasmic acyl-protein thioesterase that removes palmitate from G protein α subunits and $p21^{RAS}$. J. Biol. Chem. **273:**15830–15837.
6. **El-Husseini, A., E. Schnell, S. Dakoji, N. Sweeney, Q. Zhou, O. Prange, C. Gauthier-Campbell, A. Aguilera-Moreno, R. A. Nicoll, and D. S. Bredt.** 2002. Synaptic strength regulated by palmitate cycling on PSD-95. Cell **108:**849–863.
7. **El-Husseini, A. E.-D., and D. S. Bredt.** 2002. Protein palmitoylation: a regulator of neuronal development and function. Nat. Rev. Neurosci. **3:**791–802.
8. **Evanko, D. S., M. M. Thiyagarajan, and P. B. Wedegaertner.** 2000. Interaction with Gβγ is required for membrane targeting and palmitoylation of $G\alpha_s$ and $G\alpha_q$. J. Biol. Chem. **275:**1327–1336.
9. **Fang, C., C. A. Deng, L., Keller, M. Fukata, Y. Fukata, G. Chen, and B. Luscher.** 2006. GODZ-mediated palmitoylation of $GABA_A$ receptors is required for normal assembly and function of GABAergic inhibitory synapses. J. Neurosci. **26:**12758–12768.
10. **Fernandez-Hernando, C., M. Fukata, P. N. Bernatchez, Y. Fukata, M. I. Lin, D. S. Bredt, and W. C. Sessa.** 2006. Identification of Golgi-localized acyl transferases that palmitoylate and regulate endothelial nitric oxide synthase. J. Cell Biol. **174:**369–377.
11. **Fukata, M., Y. Fukata, H. Adesnik, R. A. Nicoll, and D. S. Bredt.** 2004. Identification of PSD-95 palmitoylating enzymes. Neuron **44:**987–996.
12. **Fukata, Y., T. Iwanaga, and M. Fukata.** 2006. Systematic screening for palmitoyl transferase activity of the DHHC protein family in mammalian cells. Methods **40:**177–182.
13. **Gilman, A. G.** 1987. G proteins: transducers of receptor-generated signals. Annu. Rev. Biochem. **56:**615–649.
14. **Huang, K., A. Yanai, R. Kang, P. Arstikaitis, R. R. Singaraja, M. Metzler, A. Mullard, B. Haigh, C. Gauthier-Campbell, C. A. Gutekunst, M. R. Hayden, and A. El-Husseini.** 2004. Huntingtin-interacting protein HIP14 is a palmitoyl transferase involved in palmitoylation and trafficking of multiple neuronal proteins. Neuron **44:**977–986.
15. **Hughes, T. E., H. Zhang, D. E. Logothetis, and C. H. Berlot.** 2001. Visualization of a functional $G\alpha_q$-green fluorescent protein fusion in living cells. Association with the plasma membrane is disrupted by mutational activation and by elimination of palmitoylation sites, but not by activation mediated by receptors or AlF_4. J. Biol. Chem. **276:**4227–4235.
16. **Jollivet, F., G. Raposo, A. Dimitrov, R. Sougrat, B. Goud, and F. Perez.** 2007. Analysis of de novo Golgi complex formation after enzyme-based inactivation. Mol. Biol. Cell **18:**4637–4647.
17. **Keller, C. A., X. Yuan, P. Panzanelli, M. L. Martin, M. Alldred, M. Sassoe-Pognetto, and B. Luscher.** 2004. The γ2 subunit of $GABA_A$ receptors is a substrate for palmitoylation by GODZ. J. Neurosci. **24:**5881–5891.
18. **Linder, M. E., and R. J. Deschenes.** 2007. Palmitoylation: policing protein stability and traffic. Nat. Rev. Mol. Cell Biol. **8:**74–84.
19. **Linder, M. E., P. Middleton, J. R. Hepler, R. Taussig, A. G. Gilman, and S. M. Mumby.** 1993. Lipid modifications of G proteins: α subunits are palmitoylated. Proc. Natl. Acad. Sci. USA **90:**3675–3679.

20. **Luttrell, L. M.** 2006. Transmembrane signaling by G protein-coupled receptors. Methods Mol. Biol. **332:**3–49.
21. **Malbon, C. C.** 2005. G proteins in development. Nat. Rev. Mol. Cell Biol. **6:**689–701.
22. **Marrari, Y., M. Crouthamel, R. Irannejad, and P. B. Wedegaertner.** 2007. Assembly and trafficking of heterotrimeric G proteins. Biochemistry **46:** 7665–7677.
23. **Ohyama, T., P. Verstreken, C. V. Ly, T. Rosenmund, A. Rajan, A. C. Tien, C. Haueter, K. L. Schulze, and H. J. Bellen.** 2007. Huntingtin-interacting protein 14, a palmitoyl transferase required for exocytosis and targeting of CSP to synaptic vesicles. J. Cell Biol. **179:**1481–1496.
24. **Oldham, W. M., and H. E. Hamm.** 2008. Heterotrimeric G protein activation by G-protein-coupled receptors. Nat. Rev. Mol. Cell Biol. **9:**60–71.
25. **Pierce, K. L., R. T. Premont, and R. J. Lefkowitz.** 2002. Seven-transmembrane receptors. Nat. Rev. Mol. Cell Biol. **3:**639–650.
26. **Prior, I. A., A. Harding, J. Yan, J. Sluimer, R. G. Parton, and J. F. Hancock.** 2001. GTP-dependent segregation of H-Ras from lipid rafts is required for biological activity. Nat. Cell Biol. **3:**368–375.
27. **Rocks, O., A. Peyker, M. Kahms, P. J. Verveer, C. Koerner, M. Lumbierres, J. Kuhlmann, H. Waldmann, A. Wittinghofer, and P. I. Bastiaens.** 2005. An acylation cycle regulates localization and activity of palmitoylated Ras isoforms. Science **307:**1746–1752.
28. **Rosethorne, E. M., S. R. Nahorski, and R. A. Challiss.** 2008. Regulation of cyclic AMP response-element binding-protein (CREB) by $G_{q/11}$-protein-coupled receptors in human SH-SY5Y neuroblastoma cells. Biochem. Pharmacol. **75:**942–955.
29. **Roth, A. F., Y. Feng, L. Chen, and N. G. Davis.** 2002. The yeast DHHC cysteine-rich domain protein Akr1p is a palmitoyl transferase. J. Cell Biol. **159:**23–28.
30. **Roth, A. F., J. Wan, A. O. Bailey, B. Sun, J. A. Kuchar, W. N. Green, B. S. Phinney, J. R. Yates III, and N. G. Davis.** 2006. Global analysis of protein palmitoylation in yeast. Cell **125:**1003–1013.
31. **Shaner, N. C., P. A. Steinbach, and R. Y. Tsien.** 2005. A guide to choosing fluorescent proteins. Nat. Methods **2:**905–909.
32. **Simon, M. I., M. P. Strathmann, and N. Gautam.** 1991. Diversity of G proteins in signal transduction. Science **252:**802–808.
33. **Smotrys, J. E., and M. E. Linder.** 2004. Palmitoylation of intracellular signaling proteins: regulation and function. Annu. Rev. Biochem. **73:**559–587.
34. **Storrie, B., J. White, S. Rottger, E. H. Stelzer, T. Suganuma, and T. Nilsson.** 1998. Recycling of Golgi-resident glycosyltransferases through the ER reveals a novel pathway and provides an explanation for nocodazole-induced Golgi scattering. J. Cell Biol. **143:**1505–1521.
35. **Stowers, R. S., and E. Y. Isacoff.** 2007. *Drosophila* huntingtin-interacting protein 14 is a presynaptic protein required for photoreceptor synaptic transmission and expression of the palmitoylated proteins synaptosome-associated protein 25 and cysteine string protein. J. Neurosci. **27:**12874–12883.
36. **Swarthout, J. T., S. Lobo, L. Farh, M. R. Croke, W. K. Greentree, R. J. Deschenes, and M. E. Linder.** 2005. DHHC9 and GCP16 constitute a human protein fatty acyltransferase with specificity for H- and N-Ras. J. Biol. Chem. **280:**31141–31148.
37. **Wedegaertner, P. B., and H. R. Bourne.** 1994. Activation and depalmitoylation of $G_s\alpha$. Cell **77:**1063–1070.
38. **Wedegaertner, P. B., D. H. Chu, P. T. Wilson, M. J. Levis, and H. R. Bourne.** 1993. Palmitoylation is required for signaling functions and membrane attachment of $G_q\alpha$ and $G_s\alpha$. J. Biol. Chem. **268:**25001–25008.
39. **Yu, J. Z., and M. M. Rasenick.** 2002. Real-time visualization of a fluorescent $G\alpha_s$: dissociation of the activated G protein from plasma membrane. Mol. Pharmacol. **61:**352–359.
40. **Zhao, L., S. Lobo, X. Dong, A. D. Ault, and R. J. Deschenes.** 2002. Erf4p and Erf2p form an endoplasmic reticulum-associated complex involved in the plasma membrane localization of yeast Ras proteins. J. Biol. Chem. **277:** 49352–49359.